Journal of the Serbian Chemical Society
JSCS-info@shd.org.rs • www.shd.org.rs/JSCS
J. Serb. Chem. Soc. *90* (0) 1–12 (2025)
JSCS–13485
Original scientific paper
Published 15 Dec 2025

Tuning crystal packing and reactivity through electrostatic and dispersion interactions: The case of phenytoin and its derivatives

IVANA S. ĐORĐEVIĆ[1]*, SONJA GRUBIŠIĆ[1], DRAGANA MITIĆ[2], DRAGAN M. POPOVIĆ[1] and NEMANJA TRIŠOVIĆ[3]

[1]*University of Belgrade, Institute of Chemistry, Technology and Metallurgy, National Institute of the Republic of Serbia, Njegoševa 12, 11001 Belgrade, Serbia,* [2]*University of Belgrade, Innovative Centre of the Faculty of Chemistry, Belgrade, Serbia and* [3]*University of Belgrade, Faculty of Technology and Metallurgy, Karnegijeva 4, 11120 Belgrade, Serbia*

(Received 5 August, revised 22 August, accepted 24 October 2025)

Abstract: Hydantoin derivatives represent a versatile class of heterocycles, known for their pharmacological properties. Because drug efficacy often depends on the fine-tuning of weak intermolecular (non-covalent) interactions, analysis of the crystal structure of a drug molecule is important, as it enables deciphering its interaction profile. In this study, the crystal packing of phenytoin and its selected derivatives were examined through dimeric motifs with different recognition modes using force-field calculations and a density functional theory (DFT) approach. The relatively polar ethoxyacetyl group at the N3 position of the hydantoin ring, capable of forming hydrogen bonds, enhances the contribution of electrostatic and polar components to the total interaction energy. In contrast, the long alkyl chain promotes hydrophobic contacts, leading to dispersion forces dominating over electrostatic interactions. The reactivity of phenytoin and its derivatives were further evaluated by examining the influence of these substituents using conceptual density functional theory (CDFT) descriptors. These findings demonstrate that substituents significantly affect crystal packing and the balance of non-covalent interactions, providing valuable insights for optimizing molecular recognition and drug–target interactions in the design of new therapeutic agents.

Keywords: intermolecular interactions; hydantoin; electron density; phenytoin; global reactivity descriptors.

INTRODUCTION

Derivatives of hydantoin (imidazolidine-2,4-dione) represent a versatile class of heterocyclic compounds with important applications in pharmacology, mater-

* Corresponding author. E-mail: ivana.djordjevic@ihtm.bg.ac.rs
https://doi.org/10.2298/JSC250805077D

ials science and crystal engineering. This five-membered ring provides conformational rigidity and planarity, facilitating interactions with biological targets (Fig. 1).

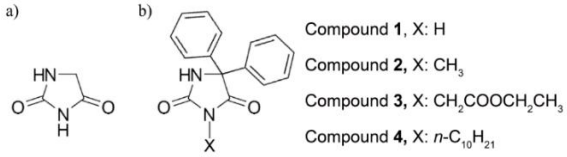

Fig. 1. Chemical structure of: a) the hydantoin and b) the phenytoin and its derivatives.

Both the carbonyl groups at positions 2 and 4 (electrophilic centres) and the NH groups at positions 1 and 3 participate in hydrogen bonding, which is crucial for interactions with biological systems. Additionally, the C5 position is a reactive methylene site suitable for functionalization. All these features contribute to the characteristic stability of hydantoin, while still providing sufficiently reactive centres for the development of new derivatives. These derivatives have a wide range of applications: in bio- and medicinal chemistry due to their pharmacological activities;[1] in agriculture as potential antimicrobial agents;[2] in coordination chemistry as valuable ligands with uses in electrochemical biosensors[3,4] and anticorrosive materials.[5] However, hydantoin derivatives are still primarily recognized for their pharmacological activities, including antimicrobial, anticonvulsant, anti-inflammatory, antidiabetic, anticancer, antiplatelet, anti-HIV and allosteric antagonist action.[1]

Phenytoin (5,5-diphenylhydantoin) is a well-known anticonvulsant drug and among the first to be developed through rational drug design.[6,7] It has been widely used for decades to manage and prevent seizures, particularly tonic-clonic and focal seizures. Disorders of the central nervous system (CNS) represent one of the major medical challenges of the twenty-first century. Despite advances in developing potential therapies for neuronal disorders, drug crossing of the blood–brain barrier (BBB) remains a significant obstacle.[8–10] Several factors influence the activity of phenytoin. It selectively blocks voltage-dependent sodium channels (NVSC) by forming hydrogen bonds, which are critical for its anticonvulsant action.[11–14] However, access to these channels depends on the presence of hydrophobic groups in the molecular structure. Such groups, particularly at the C5 position, enable hydantoins to interact with or cross the cell membrane. High lipophilicity is also important, enabling molecules to cross the BBB and remain in the brain for a longer time.[15] On the other hand, a comparison of structurally diverse hydantoin derivatives with the same log *P* values has shown that the binding affinities can vary significantly despite similar lipophilicity.[16] It appears that the orientation of the phenyl ring plays a critical role, with an optimal spatial arrangement enhancing the binding efficiency of 5-phenylhydantoins.

The crystal structure of a drug molecule plays an important role in pharmacology, as it influences solubility, stability and bioavailability (*e.g.*, different polymorphs may exhibit distinct absorption profiles). Moreover, the specific intermolecular interactions observed in the crystal structure provide valuable insights into the binding preferences of a drug molecule toward target biomolecules.[17] These features are essential for the rational design of effective and selective drugs, as well as for predicting pharmacokinetically relevant properties such as lipophilicity and membrane permeability, including the ability to cross the blood–brain barrier (BBB).

Finally, improving drug efficacy often depends on the fine-tuning of weak non-covalent (non-bonding) interactions, including polar hydrogen bonds, hydrophobic H···H contacts and van der Waals forces. These relatively weak and long-ranged interactions have a cumulative effect that makes them crucial for molecular recognition, stability and structural organization. Because accurately modelling these interactions remains challenging, modern computational methods that incorporate dispersion effects have become indispensable tools in drug design and crystal structure prediction.[18–21]

Based on the information and key issues outlined above, this study examines the intermolecular interactions in dimeric motifs extracted from the crystal packing of phenytoin and its N3-alkyl derivatives (Fig. 1). For this purpose, interaction energies of different molecular pairs were evaluated using two approaches: a force-field-based method and a density functional theory (DFT) approach. Furthermore, the influence of substituents was analysed through various descriptors, including electronegativity, hardness, and softness, within the framework of conceptual density functional theory (CDFT).

METHODOLOGY

The studied structures were obtained from the Cambridge Structural Database (CSD).[22] All calculations were carried out using Gaussian 09,[23] CrystalExplorer 21.5[24] and Mercury.[25] The interaction energies of the dimeric motifs were evaluated with the DFT-based method, at B3LYP/6-31G(d,p) level of theory, implemented in CrystalExplorer (CE-B3LYP), while the UNI force-field approach[26,27] was also applied for a comparative analysis. Both approaches rely on the same theoretical principle – the evaluation of intermolecular interaction energies – and therefore provide consistent criteria for the relevant dimers. Reported molecular pairs displayed the strongest stabilizing effects and played a representative role in describing the crystal packing motifs. Geometry optimizations of monomeric structures (compounds **1**–**4**) were carried out without constraints using the B3LYP/6-31G(d,p) level of theory in the gas phase and using the solvation model based on density (SMD) for water and dimethyl sulfoxide (DMSO), as implemented in Gaussian 09. Single-point calculations at the same level of theory were subsequently performed on the optimized geometries to obtain orbital energies in each environment. Global reactivity descriptors were then derived according to the equations provided in the Supplementary material to this paper.

RESULTS AND DISCUSSION

Structure selection

Considering the factors influencing the phenytoin activity, several of its derivatives were selected for a comparative study of preferential intermolecular interactions in their crystal packings and their molecular reactivity. Hydrogen--bond formation plays a significant role in the anticonvulsant activity of phenytoin derivatives. In contrast, hydrophobic groups at the C5 position facilitate membrane passage, enabling the molecules to reach the active site. Therefore, in addition to phenytoin, its derivatives were analysed in which the hydrogen atom at the N3 position was replaced with a methyl group, an ethoxycarbonylmethyl group, or a *n*-decyl group (Fig. 1). This selection of substituents provided structural diversity by introducing either a group capable of hydrogen bonding or short and long alkyl groups suitable for hydrophobic interactions.

Considerations of intermolecular interactions

The selected structures, extracted from the Cambridge Structural Database (CSD), crystallized in three different space groups. Compound **1**, also known as phenytoin, belongs to the orthorhombic $Pn2_1a$ space group (PHYDAN01, CCDC: 1232751).[28] Compound **2** and **4** crystallized in monoclinic $P2_1/n$ space group (PEPDUM01, CCDC: 2381918[29] and PAJMAS, CCDC: 2012925,[8] respectively). Compound **3**, which contains a polar ester group, is reported in triclinic, $P\bar{1}$ space group (JALGEL, CCDC: 1528488).[30] The most relevant dimeric motifs in the crystal packing of the investigated compounds were identified and quantitatively described, providing a deeper understanding of how molecules interact and organize within the crystal structure. For this purpose, the interaction energies of molecular pairs were determined using two distinct approaches: a DFT-based method (CE-B3LYP) and the UNI force-field energy framework. First, the results obtained with the CE-B3LYP method are discussed, followed by the corresponding energy values derived from the UNI force field.

As shown in Fig. 2 and Table S-I of the Supplementary material, the D1 and D2 motifs of compound **1**, in addition to electrostatic H···O hydrogen bonds, also exhibit significant repulsive interactions. In contrast, motifs D3, D4, D5 and D6 are predominantly stabilized by dispersion forces.

For compound **2**, electrostatic H···O interactions provide the most significant energy contribution in dimer D1, whereas dispersion interactions dominate in the other dimer motifs (Fig. 3, Table S-I).

For the dimeric motif D1 of compound **3**, the electrostatic term again dominates, and the overall interaction energy shows a remarkable increase compared to the corresponding dimers of the previous two compounds (Fig. 4, Table S-I). The symmetric arrangement of the two monomers, which feature strong N–H···O hydrogen bonds, significantly contributes to the stability of the dimeric motif D1. Dim-

ers D2, D3 and D4 exhibit a pronounced contribution from dispersion energy, accompanied by higher total interaction energies.

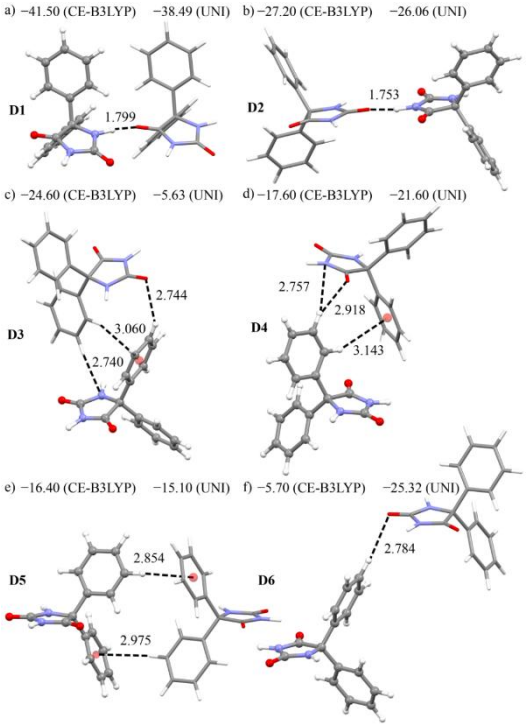

Fig. 2. Selected dimeric motifs of compound **1** with the corresponding interaction energies (in kJ mol^{-1}) calculated using the CE-B3LYP and UNI methods. The dimers were numbered according to the interaction energy values obtained from the CE-B3LYP approach. The ball-and-stick style illustrates the asymmetric unit within the dimeric motif.

Finally, although the D1 motif of compound **4** features N–H···O, C(sp^3)––H···O and C(sp^2)–H···O hydrogen bonds, dispersion interactions predominate (Fig. 5, Table S-I). A similar trend is observed for the remaining dimeric motifs, where the dispersion component dominates despite the presence of other types of interactions.

The ordering of the dimer motifs according to the interaction energies calculated with the UNI force field is mostly consistent with the results obtained using the CE-B3LYP method (Table S-I). In all studied compounds, the results for the two highest-ranked motifs are in complete agreement. Also, for compound **4**, the results from both methods correlate very well. The results presented in Table S-I reveal that the largest changes in the ranking of dimer motifs between the two methods occur for compounds **1** and **2**. For dimer D6, the interaction energy calculated using the UNI force field is significantly higher than the value obtained

with the CE-B3LYP method. For compound **3**, the UNI force field calculations indicate a perturbation in the interaction energies of the dimeric motifs D2 and D3.

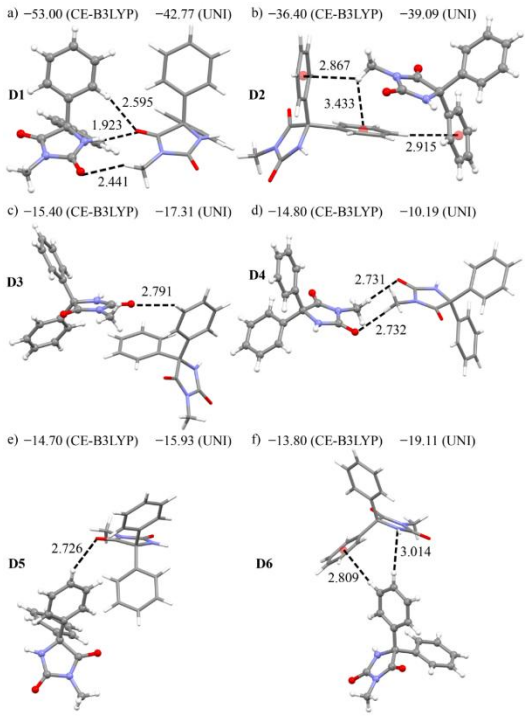

Fig. 3. Selected dimeric motifs of compound **2** with the corresponding interaction energies (in kJ mol^{-1}) calculated using the CE-B3LYP and UNI methods. The dimers were numbered according to the interaction energy values obtained from the CE-B3LYP approach. The ball-and-stick style illustrates the asymmetric unit within the dimeric motif.

The differences in dimer ranking arise because UNI (force-field) and DFT approaches estimate the relative importance of hydrogen, dispersion and electrostatic interactions differently. While DFT relies on electron density and accounts for polarization and delocalization, often highlighting polar interactions, the UNI method is purely geometric and tends to emphasize dispersive contacts.[31–33]

Reactivity profile

Conceptual density functional theory (CDFT) has evolved into a fundamental framework within quantum chemistry for predicting molecular reactivity.[34] By relating the electron density distribution and the total electronic energy of a system, CDFT provides a set of global and local descriptors that quantify molecular stability, reactivity and the location of the most reactive sites. The frontier molecular orbital (FMO) theory provides an additional approach for assessing mole-

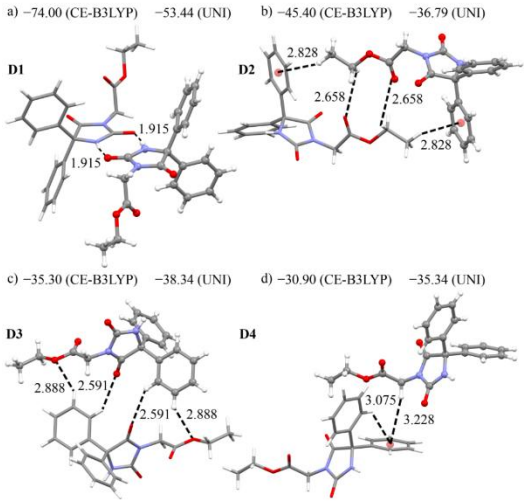

Fig. 4. Selected dimeric motifs of compound **3** with the corresponding interaction energies (in kJ mol^{-1}) calculated using the CE-B3LYP and UNI methods. The dimers were numbered according to the interaction energy values obtained from the CE-B3LYP approach.The ball-and-stick style illustrates the asymmetric unit within the dimeric motif.

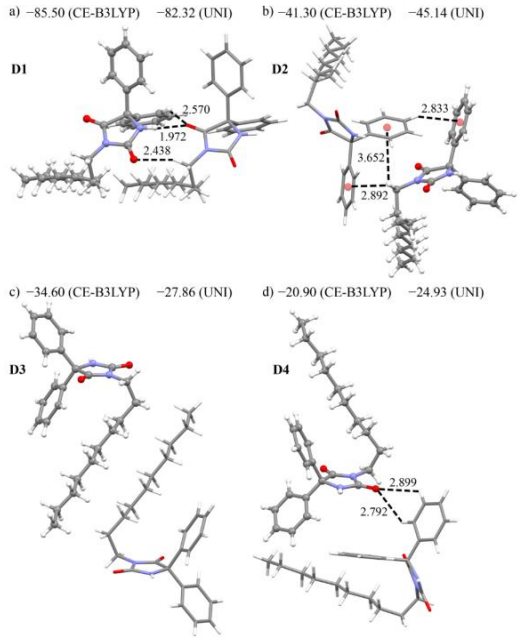

Fig. 5. Selected dimeric motifs of compound **4** with the corresponding interaction energies (in kJ mol^{-1}) calculated using the CE-B3LYP and UNI methods. The dimers were numbered according to the interaction energy values obtained from the CE-B3LYP approach. The ball-and-stick style illustrates the asymmetric unit within the dimeric motif.

cular reactivity, selectivity, and the pathways of chemical reactions.[35] The HOMO, as the highest occupied molecular orbital, typically represents an electron-rich region and acts as an electron donor in chemical interactions. In contrast, the LUMO, being the lowest-energy vacant orbital, corresponds to an electron-deficient region capable of accepting electrons. For this purpose, the FMO energies of the optimized monomeric structures were calculated in simulated environments of gas phase, water and DMSO, and subsequently used to determine the global reactivity descriptors (Table I), as defined by the equations provided in the Supplementary material.

TABLE I. The calculated energy of FMO (E_{HOMO}, E_{LUMO}), energy gap (ΔE_{gap}) and global reactivity parameters – ionization potential (*IP*), electron affinity (*EA*), chemical hardness (η), chemical potential (μ), electronegativity (χ) and electrophilicity index (ω) in units of eV for the studied compounds **1**–**4**

Compound	E_{HOMO}	E_{LUMO}	ΔE_{gap}	*IP*	*EA*	η	*M*	χ	ω
					Gas phase				
1	−6.67	−0.72	5.96	6.67	0.72	2.98	−3.70	3.70	2.29
2	−6.62	−0.66	5.96	6.62	0.66	2.98	−3.64	3.64	2.22
3	−6.55	−0.57	5.98	6.55	0.57	2.99	−3.56	3.56	2.12
4	−6.63	−0.67	5.96	6.63	0.67	2.98	−3.65	3.65	2.24
					Water				
1	−6.63	−0.79	5.85	6.63	0.79	2.92	−3.71	3.71	2.35
2	−6.62	−0.76	5.86	6.62	0.76	2.93	−3.69	3.69	2.32
3	−6.65	−0.81	5.84	6.65	0.81	2.92	−3.73	3.73	2.38
4	−6.63	−0.73	5.90	6.63	0.73	2.95	−3.68	3.68	2.30
					DMSO				
1	−6.54	−0.55	5.99	6.54	0.55	2.99	−3.55	3.55	2.10
2	−6.54	−0.54	6.00	6.54	0.54	3.00	−3.54	3.54	2.09
3	−6.55	−0.56	5.99	6.55	0.56	2.99	−3.56	3.56	2.11
4	−6.54	−0.55	5.99	6.54	0.55	2.99	−3.54	3.54	2.10

Based on the HOMO–LUMO energy gap (ΔE_{gap}) values, it can be concluded that all the studied compounds exhibit similar kinetic stability in the gas phase. Positive ionization potentials (*IP*) and similar values of chemical hardness (η) also indicate the kinetic (energetic) stability of these compounds. In compound **3**, both frontier orbital levels lie at higher energies (less negative values), which indicates reduced overall stability. Although the values of *EA*, μ, χ and ω are slightly lower in absolute terms compared to the other molecules, compound **3** is expected to show a modest overall increase in chemical reactivity.

The LUMO energy values decrease more noticeably (becoming more negative) in the simulated water environment, particularly for compound **3**. In water, the LUMO level is lowered while the HOMO remains nearly unchanged, and the chemical potential (μ) decreases, making the system more stable. As a result, both electronegativity (χ) and electrophilicity (ω) increase, indicating a stronger ten-

dency of the molecule to attract electrons and a higher reactivity toward nucleophiles. In the simulated DMSO solvent, compounds **1**, **2** and **4** become energetically less stable, less electronegative and less electrophilic, due to destabilization of the LUMO level. Therefore, its reactivity towards nucleophiles is lower in DMSO than in the gas phase.

CONCLUSION

A comparison of the results using the two methods revealed that the relative ranking of the dimers depends on the method used to evaluate interaction energies. While the energy framework based on the UNI force field relies on geometric and empirical parameters, the CE-B3LYP approach derives interaction energies directly from the electron density, explicitly accounting for polarization and charge redistribution. The DFT (CE-B3LYP) method is generally regarded as more accurate, although it can sometimes place greater emphasis on polar interactions compared to the UNI approach. Nevertheless, it is worth noting that both methods identified the key dimers with the highest interaction energies (dimers D1 and D2), providing similar values and consistent relative rankings for the dominant contributors to crystal packing. The nature and strength of intermolecular interactions in dimers are strongly influenced by the substituents. Compound **3**, bearing a polar ethoxyacetyl group, shows enhanced electrostatic and hydrogen bonding contributions, while compound **4**, with a long alkyl chain, exhibits dominant dispersion (hydrophobic) interactions. In contrast, compounds **1** and **2** with smaller or nonpolar substituents display weaker overall interactions, primarily governed by dispersion forces.

Overall, all studied compounds display comparable kinetic and energetic stability in the gas phase, with compound **3** being globally more reactive. Solvent effects are relevant for reactivity: in water, the stabilization of the LUMO enhances electrophilicity and nucleophile affinity, particularly for compound **3**, whereas in DMSO, the destabilization of the LUMO reduces these properties.

These findings highlight the critical role of substituent type in tuning molecular packing and interaction patterns in the crystal lattice, which can be utilized for the design and optimization of interactions between new drug candidates and their biological targets.

SUPPLEMENTARY MATERIAL

Additional data and information are available electronically at the pages of journal website: https://www.shd-pub.org.rs/index.php/JSCS/article/view/13485, or from the corresponding author on request.

Acknowledgements. This work was supported by the Ministry of Science, Technological Development and Innovation of the Republic of Serbia (Grants No. 451-03-136/2025-03/ /200135 and 451-03-136/2025-03/200026). We thank the COST Action CA21101 – Confined Molecular Systems: from a new generation of materials to the stars (COSY) of the European

Community for support. This research follows the United Nations 2030 Agenda for Sustainable Development Goal (SDG) 3: Good Health and Well-being.

ИЗВОД

УТИЦАЈ ЕЛЕКТРОСТАТИЧКИХ И ДИСПЕРЗИОНИХ ИНТЕРАКЦИЈА НА КРИСТАЛНУ СТРУКТУРУ И РЕАКТИВНОСТ: ПРИМЕР ФЕНИТОИНА И ЊЕГОВИХ ДЕРИВАТА

ИВАНА С. ЂОРЂЕВИЋ,[1] СОЊА ГРУБИШИЋ,[1] ДРАГАНА МИТИЋ,[2] ДРАГАН М. ПОПОВИЋ[1] и НЕМАЊА ТРИШОВИЋ[3]

[1]Универзитет у Београду, Институт за хемију технологију и металургију, Институт од националног значаја за Републику Србију, Његошева 12, 11001 Београд, [2]Универзитет у Београду, Иновациони центар Хемијског факултета, Београд и [3]Универзитет у Београду, Технолошко–металуршки факултет, Карнегијева 4, 11120 Београд

Деривати хидантоина представљају разноврсну класу хетероцикличних једињења, позната по својим фармаколошким својствима. Будући да ефикасност лека често зависи од финог подешавања слабих међумолекулских (нековалентних) интеракција, проучавање његове кристалне структуре је значајно јер омогућава разумевање његовог интеракцијског профила. У овој студији испитано је кристално паковање фенитоина и одабраних деривата анализом димера и различитих начина молекулског препознавања, коришћењем прорачуна заснованих на пољу сила (force-field) и теорији функционала густине (DFT). Релативно поларна етоксикарбонилметил-група у положају N3 хидантоинског прстена, са могућношћу успостављања водоничних веза, појачава допринос електростатичких и поларних компоненти укупној енергији интеракције. Супротно њој, дугачка алкил група подстиче успостављање хидрофобних контакта, услед чега дисперзионе силе постају доминантне у односу на електростатичке интеракције. Реактивност фенитоина и његових деривата додатно је испитана коришћењем дескриптора концептуалне теорије функционала густине (CDFT). Резултати показују да супституенти значајно утичу на изградњу кристалног паковања и природу нековалентних интеракција, пружајући притом значајан увид за разумевање молекулског препознавања и интеракција молекула лека са циљним местима што даље доприноси дизајнирању нових терапијских агенаса.

(Примљено 5. августа, ревидирано 22. августа, прихваћено 24. октобра 2025)

REFERENCES

1. S. Cho, S.-H. Kim, D. Shin, *Eur. J. Med. Chem*. **164** (2019) 517 (https://doi.org/10.1016/j.ejmech.2018.12.066)
2. W. Liu, S. Zhang, L. Xiao, Y. Wan, L. He, K. Wang, Z. Qi, X. Li, *Pest Manage. Sci*. **78** (2022) 1438 (https://doi.org/10.1002/ps.6761)
3. R. Rayhan, Md. S. H. Shishir, Md. A. Khaleque, Md. R. Amin, Md. R. Ali, M. A. S. Aly, S. M. Ayon, R. Saidur, T. H. Kim, Md. A. Zaed, Md. Z. Hossain, *RSC Adv*. **15** (2025) 24917 (https://doi.org/10.1039/D5RA03128A)
4. K. Kaewket, K. Ngamchuea, *RSC Adv*. **13** (2023) 33210 (https://doi.org/10.1039/D3RA06175B)
5. E. D. Akpan, O. Dagdag, E. E. Ebenso, *Coord. Chem. Rev*. **489** (2023) 215207 (https://doi.org/10.1016/j.ccr.2023.215207)
6. L. L. Brunton, B. C. Knollmann, *Goodman & Gilman's Pharmacological Basis of Therapeutics*, 14th ed., L. L. Brunton, B. C. Knollmann, Eds., McGraw-Hill, New York, 2022, p. 1664 (ISBN 978-1264258079)

7. M. Rask-Andersen, M. Almén, H. Schiöth, *Nat. Rev. Drug. Discov.* ***10*** (2011) 579 *(*https://doi.org/10.1038/nrd3478*)*
8. W. Guerrab, El Jemli Meryem, A. Jihane, D. Güneş, T. M. Joel, T. Jamal, I. Azeddine, A. M'Hammed, A. Katim, R. Youssef, *J. Biomol. Struct. Dyn.* **40** (2021) 8765 (https://doi.org/10.1080/07391102.2021.1922096)
9. A. Domínguez, A. Álvarez, B. Suárez-Merino, F. Goñi-de-Cerio, *Rev. Neurol*. **58** (2014) 213 (https://pubmed.ncbi.nlm.nih.gov/24570360/)
10. H. L.Wong, X. Y. Wu, R. Bendayan, *Adv. Drug Deliv. Rev*. **64** (2012) 686 (https://doi.org/10.1016/j.addr.2011.10.007)
11. N. Trišović, N. Valentić, G. Uščumlić, *Chem. Cen. J.* **5** (2011) 62 (https://doi.org/10.1186/1752-153X-5-62)
12. J. R. Smythies, in *Progress in Drug Research*, G. H. Glaser, J. K. Penry, J. Kiffin, D. M. Woodbury, Eds., Raven, New York, 1980, p. 207
13. N. Trišović, N. Valentić, M. Erović, T. Đaković-Sekulić, G. Uščumlić, I. Juranić, *Monatsh. Chem.* **142** (2011) 1227 (https://doi.org/10.1007/s00706-011-0639-7)
14. N. Trišović, T. Timić, J. Divljaković, J. Rogan, D. Poleti, M. M. Savić, G. Uščumlić, *Monatsh. Chem.* **143** (2012) 1451 (http://dx.doi.org/10.1007/s00706-012-0791-8)
15. W. M. Pardridge, *Curr. Opin. Pharmacol.* **6** (2006) 494 (https://doi.org/10.1016/j.coph.2006.06.001)
16. M. L. Brown, G. B. Brown, W. J. Brouillette, *J. Med. Chem*. **40** (1997) 602 (https://doi.org/10.1021/jm960692v)
17. P. R. Spackman, L. J. Yu, C. J. Morton, M. W. Parker, C. S. Bond, M. A. Spackman, D. Jayatilaka, S. P. Thomas, *Angew. Chem. Int. Ed.* **58** (2019) 16780 (https://doi.org/10.1002/anie.201906602)
18. M. Stöhr, T. Van Voorhis, A. Tkatchenko, *Chem. Soc. Rev*. **48** (2019) 4118 (https://doi.org/10.1039/C9CS00060G)
19. D. Wu, D. G. Truhlar, *J. Chem. Theory Comput*. **17** (2021) 3967 (https://doi.org/10.1021/acs.jctc.1c00162)
20. C. Tantardini, A. A. L. Michalchuk, A. Samtsevich, C. Rota, A. G. Kvashnin, *Sci. Rep.* **10** (2020) 7816 (https://doi.org/10.1038/s41598-020-64261-4)
21. S. Tretiakov, A-K. Nigam, R. Pollice, *Chem. Rev*. **125** (2025) 5776 (https://doi.org/10.1021/acs.chemrev.4c00893)
22. C. R. Groom, I. J. Bruno, M. P. Lightfoota, S. C. Ward, *Acta Crystallogr., B* **72** (2016) 171 (https://doi.org/10.1107/S2052520616003954)
23. *Gaussian 09 (revision D.01)*, Gaussian, Inc., Wallingford, CT, 2009
24. P. R. Spackman, M. J. Turner, J. J. McKinnon, S. K. Wolff, D. J. Grimwood, D. Jayatilaka, M. A. Spackman, *J Appl. Cryst*. **54** (2021) 1006 (https://doi.org/10.1107/s1600576721002910)
25. C. F. Macrae, I. Sovago, S, J. Cottrell, P. T. A. Galek, P. McCabe, E. Pidcock, M. Platings, G. P. Shields, J. S. Stevens, M.Towler, P. A. Wood, *J. Appl. Cryst*. **53** (2020) 226 (https://doi.org/10.1107/S1600576719014092)
26. A. Gavezzotti, *Acc. Chem. Res*. **27** (1994) 309 (https://doi.org/10.1021/ar00046a004)
27. A. Gavezzotti, G. Filippini, *J. Phys. Chem*. **98** (1994) 4831 (https://doi.org/10.1021/j100069a010)
28. K. Chattopadhyay, R. A. Palmer, J. N. Lisgarten, *J. Crystallogr. Spectrosc. Res*. **23** (1993) 149 (https://doi.org/10.1007/BF01195449)
29. W. Guerrab, R. Akrad, M. Ansar, J. Taoufik, J. T. Mague, Y. Ramli, *IUCrData* **2** (2017) x171534 (https://doi.org/10.1107/S2414314617015346)

30. Y. Ramli, R. Akrad, W. Guerrab, J. Taoufik, M. Ansar, J. T. Mague, *IUCrData* **2** (2017) x170098 (https://doi.org/10.1107/S2414314617000980)
31. M. J. Turner, S. P. Thomas, M. W. Shi, D. Jayatilaka, M. A. Spackman, *Chem. Comm*. **51** (2015) 3735 (https://doi.org/10.1039/C4CC09074H)
32. M. A. Spackman, D, Jayatilaka, *CrystEngComm* **11** (2009) 19 (https://doi.org/10.1039/B818330A)
33. C. F. Mackenzie, P. R. Spackman, D. Jayatilaka, M. A. Spackman, *IUCrJ* **4** (2017) 575 (https://doi.org/10.1107/S205225251700848X)
34. P. Geerlings, F. De Proft, W. Langenaeker, *Chem. Rev*. **103** (2003) 1793 (https://doi.org/10.1021/cr990029p)
35. P. Politzer, F. Abu-Awwad, *Theor. Chem. Acc*. **99** (1998) 87 (https://doi.org/10.1007/s002140050307).